Tunable Solid-State Properties and Anisotropic Charge Mobility in Hydrogen-Bonded Diketopyrolopyrrole Polymers Through High-Throughput Automation

Audithya Nyayachavadi,[1†] Chengshi Wang[3†], Aikaterini Vriza[3], Yunfei Wang,[2] Madison Mooney,[1] Gage T. Mason,[1] Yuzi Liu,[3] Xiaodan Gu,[2] Henry Chan[3], Jie Xu*[3] and Simon Rondeau-Gagné*[1]*

[1] Department of Chemistry and Biochemistry, University of Windsor, Ontario, Canada N9B 3P4
[2] School of Polymer Science and Engineering, The University of Southern Mississippi, Hattiesburg, MS 39406, USA
[3] Nanoscience and Technology Division, Argonne National Laboratory, Lemont, IL, USA

Abstract

The optoelectronic properties and device performance of organic semiconducting polymers relies on a delicate interplay of material chemical structure, noncovalent solid-state interactions, and processing conditions. However, screening, understanding, and optimizing the relationships between these parameters for reliably fabricating high performance organic electronics is an arduous task requiring significant time and resources, often hindering the development of new technologies that address contemporary socio-economic and environmental challenges. Towards addressing this limitation, we report the usage of a robotically automated device fabrication and characterization platform capable of producing organic field-effect transistors (OFETs) through the solution processing and subsequent blade-coating of various π-conjugated semiconducting polymers. Named "Polybot", this automated platform is capable of high-throughput fabrication and electronic measurements of OFETs, allowing for mass acquisition and subsequent analysis of data to uncover novel material property relationships for further refinement of rational chemical design and processing conditions. To demonstrate the prowess of this platform, this work investigates novel hydrogen bonding containing diketopyrolopyrrole (DPP)-based polymer for thin film blade-coated OFET fabrication. Through high-throughput fabrication of analysis, interesting data trends were analyzed, namely control over the extent of anisotropic charge

mobility (ranging from a anisotropy ratio of 1 to over 690) can be observed in thin films. The materials and resulting films were thoroughly characterized using a combination of techniques including cryo-electron microscopy, polarized UV-Vis spectroscopy, atomic force microscopy (AFM), X-ray scattering, and polarized optical microscopy to understand the role of processing conditions in solid-state and electronic properties of these organic semiconductors. Overall, these findings demonstrate that the use of automated fabrication and characterization platforms can provide valuable insights into optimization and uncovering the potential of novel electroactive materials, ultimately leading to new avenues and insights towards designing high performance next generation technologies.

Introduction

Organic semiconductors, particularly π-conjugated polymers, have become an established platform for designing next-generation soft technologies for biomedical, advanced manufacturing and energy production.[1–4] The diversity and effectiveness of electroactive materials stem from the broad spectrum of molecular structures achievable through careful chemical design and processing methods. These tailored approaches enable the production of materials with specific characteristics, including fluorescence, mechanical flexibility, self-healing features, and compatibility with environmentally-friendly solvents.[5–8] Particularly, the constant evolution of donor-acceptor conjugated polymers has resulted in material designs that have surpassed the performance of amorphous silicon, with charge carrier mobilities now surpassing 10 $cm^2V^{-1}s^{-1}$ in organic field-effect transistors (OFETs). Although significant advancements have been made, the intricate interplay among chemical design, materials processing, and thin film morphology for high-performance organic electronics is not fully comprehended. Moreover, it has been

consistently shown through past literature that each aspect of the device fabrication process is crucial for developing high-quality, stable organic electronics.[9,10]

When investigating from the perspective of chemical design, the strategy of side-chain engineering, where the solubilizing alkyl groups typically required on these polymers to ensure solubility in common organic solvents are synthetically modified, has become the *de facto* approach for modulating the optoelectronic, solid-state and mechanical properties of conjugated polymers.[11,12] To advance conjugated polymer research, researchers have extensively adopted an Edisonian approach—characterized by extensive trial-and-error experimentation. This has led to the exploration of various side-chain motifs, including ligands, perfluorinated groups, oligosiloxanes, and natural product derivatives.[13–16] These design elements have been integrated into the chemical structures of high-performance conjugated polymers with the aim to enable desirable properties to the materials, including stretchability, self-healing, and environmentally-friendly processability.[15,17–20] In addition to these, there has been an increasing tendency for utilizing hydrogen bond containing side chains as they have shown to help promote solid-state self-assembly, enhance mechanical properties, enable intrinsic self-healing, and alter solubility and processing conditions of the semiconducting polymers.[21–23] Furthermore, the incorporation of hydrogen bonding moieties can impact the optoelectronic properties of conjugated polymers, thus offering additional avenues for materials design.[24,25] Despite the many instances of semiconducting polymers that incorporate hydrogen bonding moieties, the core effects of these components on materials processing and the overall bulk properties of the polymers are not completely understood.[26] Additionally, there is a vast, unexplored potential in optimizing these hydrogen bonding interactions. Exploring this area by characterizing and identifying the new

properties that emerge from various solution processing techniques, present a significant opportunity for materials discovery and organic electronics optimization.[27]

The transitionary mindset when moving from a chemical design space to the material processing and device engineering space invokes some unique challenges. Thanks to years of synthetic and computational advances, designing promising chemical structures and simulating the properties of individual polymer chains with novel designs has become quite feasible. However, predicting their processability and behavior in electronic devices remains a significant challenge. This difficulty arises from the multitude of factors that play a role in what is known as device optimization. These numerous parameters make it complex to foresee how these materials will perform in practical applications.[28] Optimizing organic materials for more performant organic electronics relies on a complex yet delicate interplay of chemical structure design, solvent processing selection, and choice of device fabrication technique, and fabrication environment.[29–31] In this context, the use of automation for device fabrication offers some unique advantages, namely the faster screening of coating conditions (i.e., blade coating velocity and substate temperature) as well elimination of human variance during device fabrication. Thus, through automated processing and device fabrication, it can be possible to investigate and ultimately understand the parameters involved with the electronic performance of conjugated polymers and truly understand the full capabilities of material synthetic design.

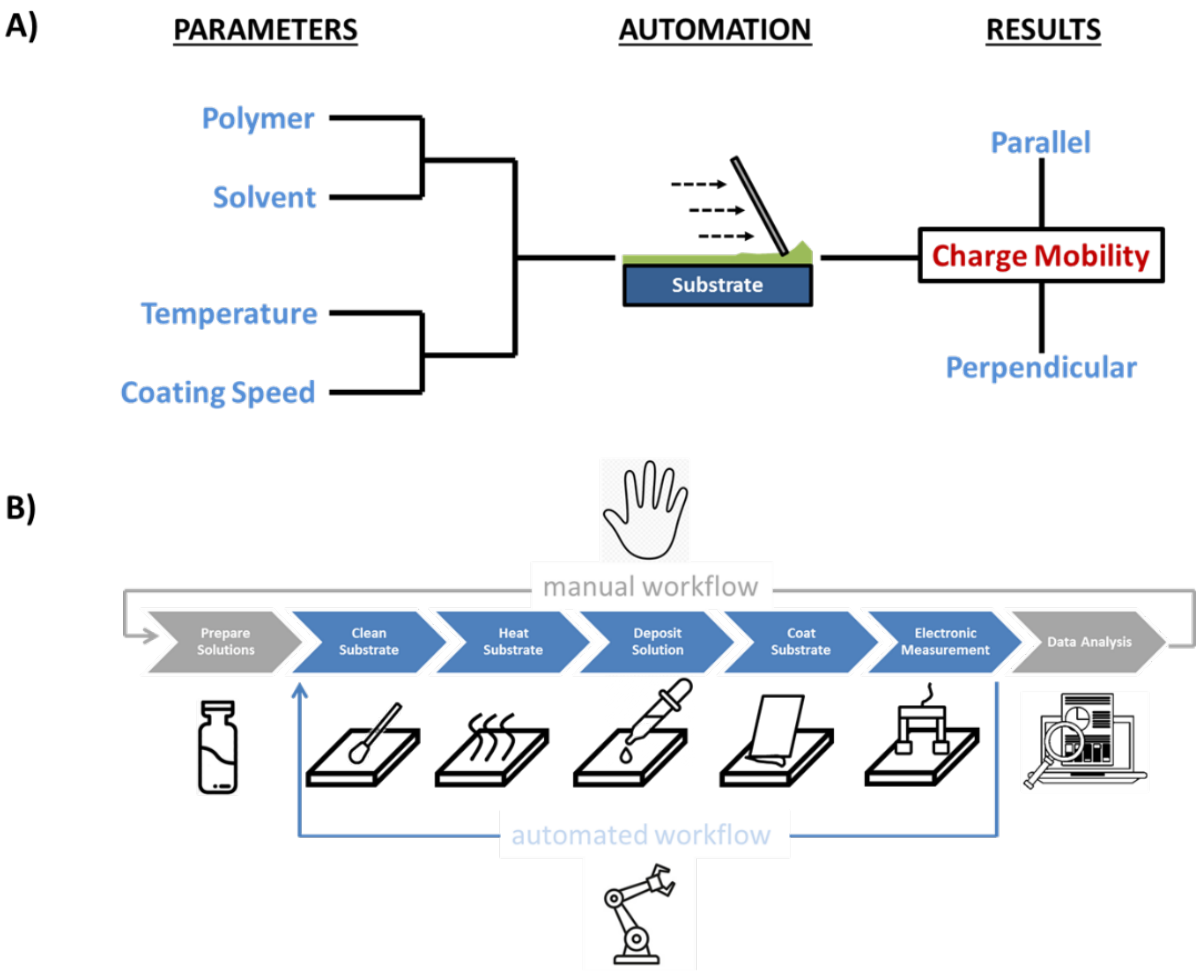

Figure 1. A) Representative workflow of the automated device fabrication and data measurement/acquisition of the Polybot platform for OFET devices. A polymer design of choice is dissolved in a suitable solvent, where a two-dimensional study is conducted based on blade-coating, where annealing temperature and blade-coating speed are selected for by the robotic AI. Through automation, the devices are fabricated and analyzed to look at charge carrier mobility of the resulting polymer thin films. B) The automated workflow of Polybot for the fabrication and electrical measurement of bottom-gate bottom-contact OFETs. Solutions of polymer are pre-prepared at 10mg/mL and then integrated into the robotic platform. Pre-patterned n-doped silicon substrates with gold electrodes are cleaned by the robot, followed by heating to a specific temperature that is less than the boiling point of the specific solvent, specifically $CHCl_3$ in this experiment. Upon reaching a temperature chosen by the robot's AI, the polymer solution is then deposited and subsequently coated across the substrate using an OTS-functionalized blade that moves at a velocity chosen by the robot's AI. The substrate then has its charge carrier mobility measured by the robot using a probe station, which is subsequently analyzed as a mobility value in both the parallel and perpendicular directions to the blade coating vector.

Herein, we report the use of a unique automated platform, so-called "Polybot" investigate the influence of hydrogen bond driven self-assembly on the processing of semiconducting polymers, and to explore and better understand their impact on the materials electronic properties in OFETs. More precisely, this work focuses on a DPP-based conjugated polymer with side chains moieties that can generate intermolecular hydrogen bonding, processed through automated blade-coating from a solution (Figure 1b). A diverse set of processing conditions were systematically varied, specifically focusing on adjusting substrate temperature and blade-coating speed. This approach facilitated the collection of a large dataset of charge mobility measurements from the fabricated OFETs. The analysis of these measurements provided insights into a range of electronic phenomena and performance characteristics. A key finding from this high-throughput experimental approach was the ability to control the degree of anisotropic charge transport in the OFETs by carefully altering the fabrication conditions. This control over anisotropic charge transport led to a more in-depth examination. Selected thin films, produced under specific conditions that demonstrated varied degrees of anisotropic charge transport, were extensively analyzed to explore, and understand the relationship between the solid-state properties of the materials (arising from the chosen fabrication conditions) and their anisotropic charge transport behaviors. Notably, through evaluation of polarized optical microscopy, grazing-incidence wide-angle X-ray scattering (GIWAXS), and polarized UV-vis spectroscopy, it was found that factors such as crystallinity, amorphous chain alignment and dipole transition alignment in the hydrogen bond containing polymer can be directly correlated to the degree of anisotropic charge transport observed in correlated devices, providing a potential future avenue for designing low-cost technologies where anisotropic characteristics are relevant such as sensors, displays and optical communication. Ultimately, our results show that using a high-throughput experimentation by

varying device fabrication conditions, particularly substrate temperature and blade coating velocity can result in vast changes in electronic performance of materials while also resulting in uncovering novel electronic properties, moving closer to the discovery of the full potential of a functional polymer.

Results and Discussion

For this work, amide-containing conjugated polymers were used due to several key reasons. First, amides can be synthetically easily. Furthermore, previous work from our group and others demonstrated that, when incorporated in small molar fractions, amide functional groups can have significant impact on semiconducting polymers, particularly on charge transport and mechanical properties.[32,33] Notably, amide-containing side-chains have been shown to intrinsically induce pre-aggregation of semiconducting polymers in solution, often resulting in the formation of well-defined solid-state morphologies upon deposition.[26] This feature is particularly desirable for blade-coating since the formation of such aggregates can result in highly aligned polymer chains in thin films, thus leading to enhanced mechanical properties and electronic performance. Currently, strategies to induce pre-aggregation in the solution state for blade-coating has involved investigating parameters such as the use of nucleation agents, co-solvent blending, sonication, solution and UV-induced degradation, and specialized equipment and substrates.[34,35]

Automating a blade-coating experiment involves careful consideration of various logistical aspects. First, the selection and setup of appropriate equipment are crucial; this includes choosing a reliable robotic arm or automated system capable of precise movements for measuring and transport of coating solutions to the desired substrate. The automation process also requires the development of a well-defined workflow, including the pre-preparation of coating materials, loading, and unloading of pre-patterned substrates, and careful control of fabrication conditions

such as temperature blade-coating velocity. Finally, integration of electronic probes capable of carrying automated electronic measurements, in this case hole charge carrier mobility, are also a necessity to fully realize the workflow.

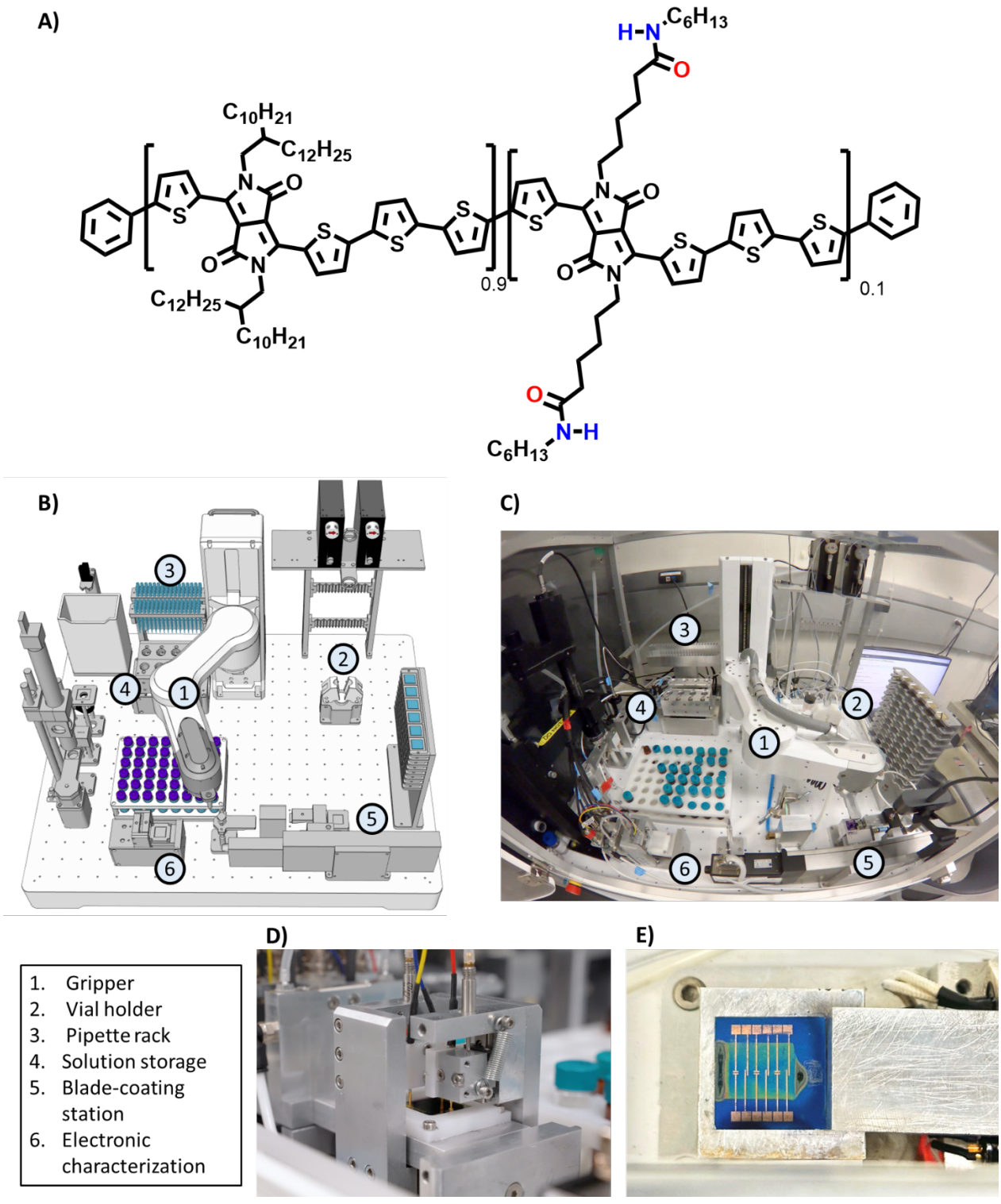

Figure 2. Polybot automated platform used for the processing and characterization of OFETs. A) Chemical structure of the hydrogen-bond containing DPP conjugated polymer. B) Simulation of the robot stations and tools used for the OFET workflow C) Actual image of the real station D) Zoomed vile of the coating station E) Zoomed view of the OFET film after blade coating.

As shown in **Figure 2b** and **Figure 2c**, the Polybot platform is composed of six key hardware components for automating the experimental workflow. The gripper robotic arm (1) serves as the main transport mechanism of the platform and is responsible for the bulk of the automated workflow; through this *n*-doped silicon substrates with pre-patterned gold electrodes are moved from the substrate rack to the blade coating station (5), which is equipped with a heating mantle to heat the substrate to a selected temperature by the robot, which a limitation being placed on the software to ensure that the temperature is not within 5°C of the boiling point of the solvent, in this case $CHCl_3$. Next, the gripper moves to the vials of pre-prepared solutions from the solution rack which are subsequently transferred to the vial holder (2), upon which they are uncapped. Following this, the gripper moves to the pipette rack (3) to attach itself with a disposable pipette tip, which then moves to the uncapped vial in the vial holder to draw a set amount of polymer solution from the vial and is then moved to the blade-coating station to dispense the solution on the substrate functionalized with a phenyltrimethoxysilane (PTS) monolayer which then coats the solution at a velocity determined by the robotic platform (**Figure 2d**) on the final substrate (**Figure 2e**). Simultaneously, the gripper arm moves back to the vial holder to re-cap the vial to mitigate excessive solvent evaporation. Finally, the coated substrate is picked up by the gripper and moved to the electronic characterization station (6), upon which tungsten probes are placed in contact with the substrate to measure device characteristics through the recording of current-voltage and output characteristic curves. It is to note that as shown in **Figure 2e**, the pre-patterned gold electrodes are specifically designed to measure device characteristics both parallel and perpendicular to the direction of blade-coating, as it has been demonstrated in previous reports that significant differences in the charge mobility can be observed based on the measurements taken with respect to the vector of the coating direction. Upon completion of measurements and data storage, the

robot moves the substrate back to the substrate-holding rack and the OTS-functionalized blade is cleaned with a toluene (jet integrated into the blade coating apparatus) to remove any residue on the blade for the next experiment cycle. The entire workflow experiment is carried out in a sealed plastic box with a door and an inlet of argon gas to work under inert atmosphere as much as possible. Upon completion of the set determined number of experimental cycles (or complete use of solution), the gripper moves the capped vial back to the vial storage rack. Furthermore, all experiments are formed are replicated in duplicate to ensure accuracy and reproducibility. Through this automated workflow, over 30 separate workflow experiments (60 in total) were run within 48 hours, demonstrating the power of automation to uncover a large experimental space within a time and cost-effective manner.

To explore the experimental capabilities of the Polybot platform, we selected two key variables for analysis, i.e., the substrate coating temperature and the blade velocity, through a constrained random sampling method/ controlled design of experiments method. The temperatures were varied from 30 to 50^{o}C in increments of 5^{o}C, while the blade velocity was adjusted from 0.5 to 50 mm/s with a step of 0.5 mm/s. Our selection was strategically biased towards higher temperatures, given the increased solubility of the polymer at these ranges, and towards lower blade speed, as previous experiments have shown these conditions to favor film uniformity. By doing so, the robot was able to screen for a variety of blade-coating conditions to generate a significant body of data for investigating the charge mobility of the hydrogen-bond containing polymer in relation to the device fabrication conditions, as visualized in **Figure 3**.

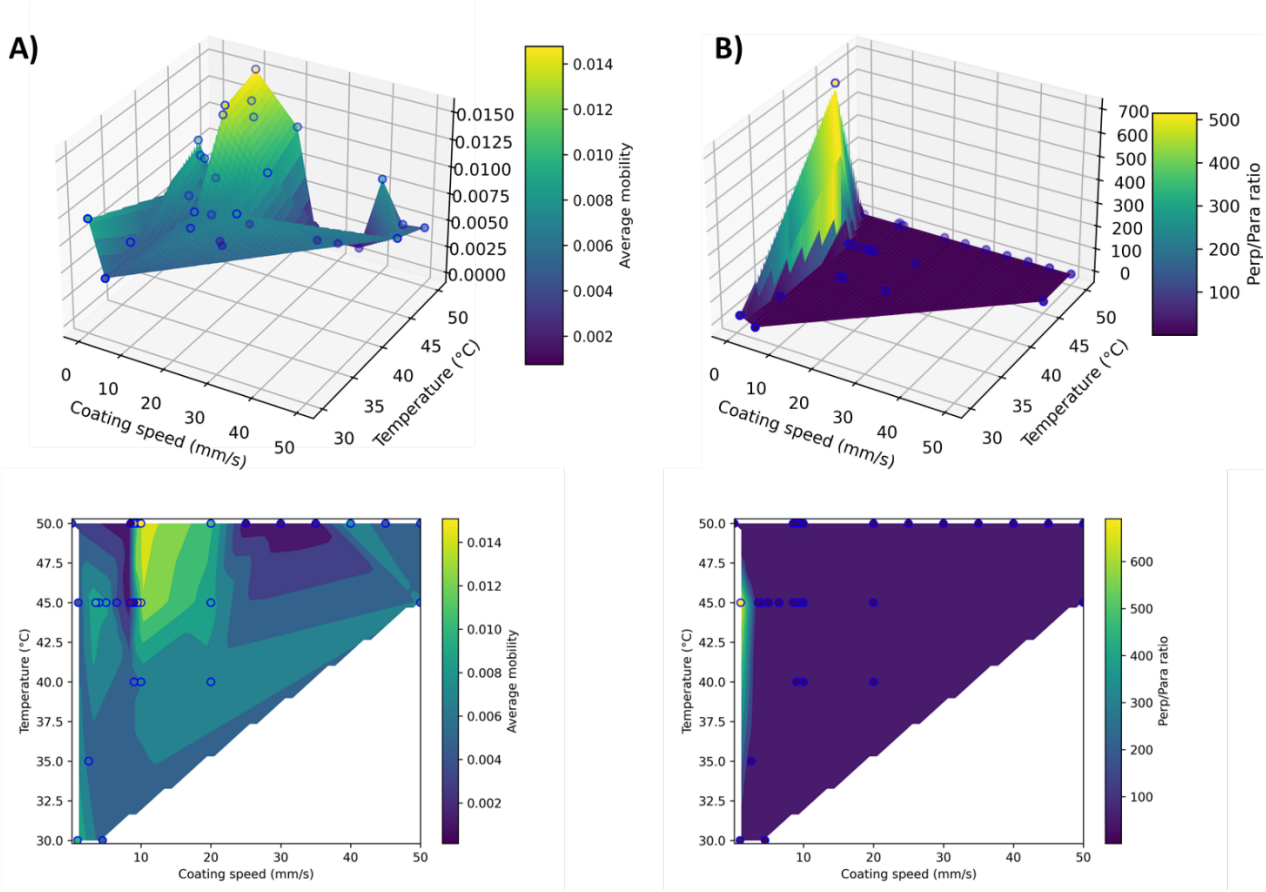

Figure 3. Experimental visualization of the 30 different experimental conditions (circles) regarding the blade-coating of **P1** ran through the Polybot Interface. A) 3D (top) and 2D (bottom) surface response of the Average mobility towards the experimental conditions. B) 3D (top) and 2D (bottom) surface response of ratio of perpendicular to parallel mobility towards the experimental conditions. The linear interpolate module from SciPy library was used to interpolate the scattered data onto a uniform grid. The grids are color-coded based on the average mobility and perpendicular to parallel mobility ratio respectively.

First, device characteristics were evaluated. Directly performed by Polybot, transfer and output curves were measured for all devices, with representative curves shown in Figures XX and XXX. The charge carrier mobility was extracted from the transfer curves through linear fitting of $I_{DS}^{1/2}$ *vs.* V_{GS} in the saturation regime using $I_{DS(sat)}=(WC/2L)\mu_{sat}(V_G - V_{th})^2$. Since some of the transfer curves exhibited slight non-linearity, a slope of $I_{DS}^{1/2}$ *vs.* V_{GS} from approximately V_{GS} = -15V to -55V was used to avoid over- or underestimation of mobilities.[36] Charge carrier mobility

was measured in two directions, parallel and perpendicular to the direction of blade-coating to understand the anisotropic implications with the coating technique. Furthermore, the average charge mobility, calculated from both perpendicular and parallel charge mobilities, was also evaluated to provide a comprehensive view of the electronic properties of the semiconducting materials in thin films.

Towards obtaining an overall view of the electronic properties of the polymer, the impact of temperature and blade-coating based processing on the overall average mobility, the average thin film mobilities were 3D and 2D mapped as shown **Figure 3A**. Through the high-throughput experimentation, we observed that higher average mobility values were displayed at coating speeds that ranged from 10 mm/s to 20 mm/s and at elevated temperatures, with the highest average mobility value being measured at 0.0151 $cm^2V^{-1}s^{-1}$, occurring at 10mm/s at a temperature of 50°C. Conversely, the lower range of mobilities observed were at coating speeds beneath the 10mm/s range (such as 0.00166 $cm^2V^{-1}s^{-1}$ at 6.5 mm/s), and between 25-35 mm (such as 0.000666 $cm^2V^{-1}s^{-1}$ at 30 mm/s). It is noted that with blade-coating, the velocity at which the coating occurs significantly impacts factors such as chain alignment and film crystallinity, all of which play a role in charge transport, but the optimal speed can be unique for each material, thus automated high throughput screening is advantageous for optimizing this processing parameter.[27,37] More broadly, it was also noted that higher substrate temperatures, closer to the boiling point of $CHCl_3$, also resulted in higher mobilities, but this trend was not as defined. However, it was observed that small changes in coating temperature, such as the difference between 45°C and 50°C, resulted in generally higher mobility values on average, indicating that electronic performance of the thin films are significantly sensitive to temperature conditions. While the reasoning for this requires further investigation, it is known that hydrogen bond driven self-assembly is sensitive to

temperature changes, which could be a contributing factor to this observation.[38] Thus, further analysis would entertain exploring smaller temperature shifts (i.e. 1°C ranges instead of the 5°C used for this experiment) for further optimization and understanding of thin film electronic properties. Overall, the average mobilities obtained from the blade-coated experiments fall within the range of previously reported BGBC films, ranging in magnitude from 10^{-2} to 10^{-5} $cm^2V^{-1}s^{-1}$, with a comprehensive list of these values shown in Table S2. Furthermore, these values agree with previously reported amide containing DPP polymers previously reported by our group and others.[39–41] While there are few examples of other hydrogen bond containing polymers that led to higher performance in OFETs, it is important to note that the value obtained through Polybot have been measured under ambient conditions in absence of a controlled environment, which is known to significantly impact the magnitude of mobilities.[42]

By meticulously analyzing the data obtained from these experiments, particularly when placing special attention to the results obtained under different coating speed at elevated temperatures, we observed a significantly broad range of anisotropy in charge mobility measured, providing hints at a potential direct influence of the hydrogen bond-containing sidechains. Defined as the ratio in charge carrier mobility between the parallel blade-coating direction to the perpendicular one, charge mobility anisotropy is a particularly desirable characteristic in organic electronics due to its contribution to directionally enhanced mechanical and optoelectronic properties. This trait is especially valuable in the fabrication of large transistor arrays, where it plays a crucial role in minimizing parasitic current leakage between adjacent arrays. Effective control of this leakage is essential for the optimal performance and durability of these devices, making anisotropic properties a key focus in advancing organic electronic technologies.

When investigating the charge carrier anisotropy of the films, as depicted in **Figure 3B**, it was observed that higher anisotropy occurred at lower coating speeds, particularly under 10 mm/s, indicating that lower velocities favor greater alignment within the hydrogen containing polymer system, as per Table S2. Notably, the highest anisotropic ratio measured in the set of experiments at 690.60 (0.004519 $cm^2V^{-1}s^{-1}$ in the parallel direction versus $6.54E^{-06}$ $cm^2V^{-1}s^{-1}$ in the perpendicular direction) occurred at a coating speed of 1mm/s at a temperature of 45°C, further demonstrating that at lower speeds, greater alignment can occur due to kinetic trapping effects, thus resulting in more directional mobilities.[43] However, it was noted that at a coating speed of 0.1 mm/s as per Table S1, no significant anisotropy was observed, indicating that even lower speeds might not be beneficial for chain alignment. This could also be potentially attributed to the volatility and vapor pressure of $CHCl_3$ resulting in poor film quality and evaporation as the blade moves, thus future work can look at investigating higher boiling point solvents to mitigate these effects and further analyze sub-1 mm/s coating speeds.

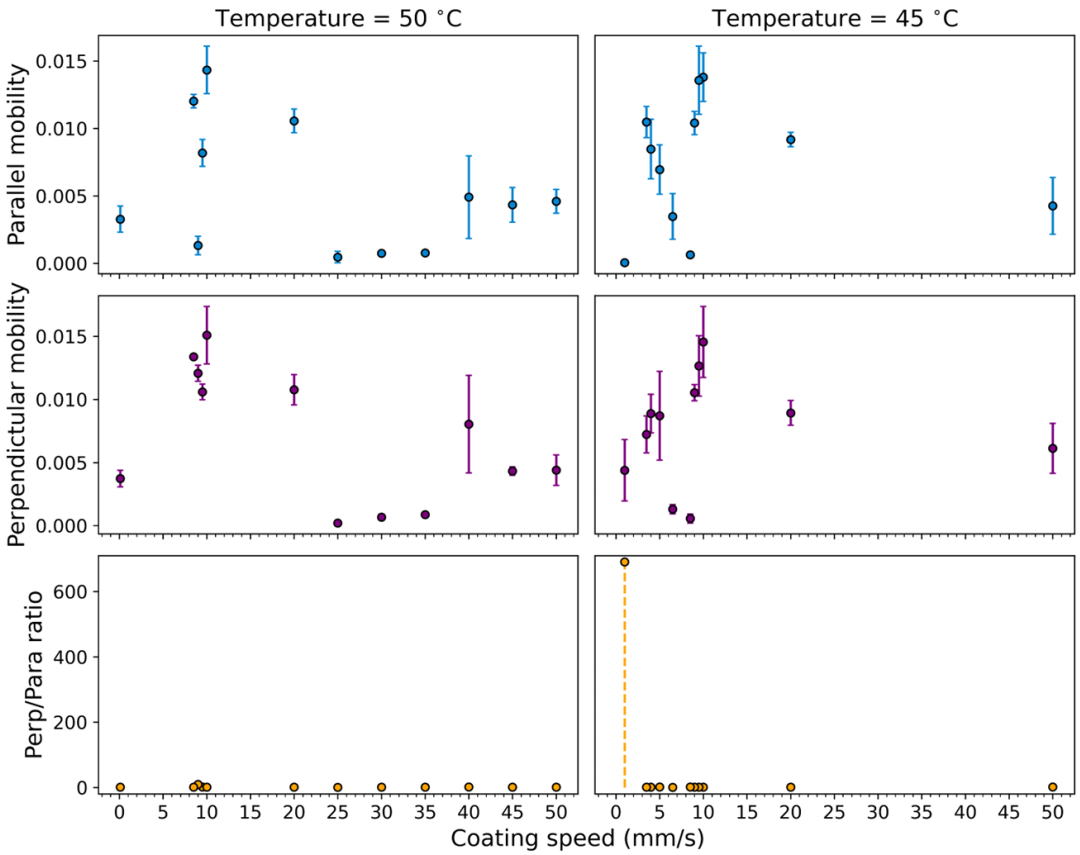

Figure 4. Visual data extrapolation of data and tends associated with elevated coating temperatures within the Polybot. In the experimental space analyzed by the robot, charge anisotropy was discovered as an important phenomenon that arise from the blade-coating of the hydrogen bonding containing polymer.

Interestingly, a correlation between substrate coating temperature and anisotropic electronic properties was also observed. On average at elevated temperatures, as highlighted in Figure 4, it was found these higher ranges, namely 45°C and 50°C, would more consistently result in anisotropic charge transport values, particularly at coating speeds beneath 10 mm/s. This is consistent with previous reports that suggest that higher temperatures can induce crystallization and alignment effects in extended conjugated and hydrogen bond containing systems, which when combined with suitable blade coating speeds can result in self-assembled and highly aligned morphologies.[44,45] However, it was observed that at higher coating speeds, these elevated

temperatures proved no correlation to charge anisotropic character, indicating there are limitations to temperature induced effects within this polymer system with regards to anisotropy. A possible explanation for this observation is the combination of elevated temperatures in conjunction with the higher speeds of the blade might provide sufficient force to disrupt the hydrogen bonding interactions associated with the amide motif, resulting in the hydrogen bonding no longer contributing to anisotropic alignment.

Overall, this observed anisotropic phenomenon indicates that the presence of moieties capable of generating intermolecular hydrogen bonding, when combined with a meticulous processing optimization, can allow for the controlled formation of a well-defined nanoscale morphology in the solid-state without relying on additives, elaborate processing conditions, or the use of complex solvent systems or blends, which are traditionally required to achieve chain alignment.[31] Furthermore, the potential for controlling both the degree of electronic performance as well as alignment through simple processing conditions afforded by a material's intrinsic chemical properties, namely hydrogen bonding, opens the door for applications for applications where materials with multifunctional properties and domains are required, such as artificial skin and augmentation.[46]

Using Polybot for screening a variety of parameters, and through selection of specific results, we further investigated trends for understanding the implication of hydrogen bond containing side chains on electronic properties, particularly in this case charge anisotropy and understand the role of structural property relationships. Notably, out of the 30 conditions, 6 conditions exhibited were selected for further analysis that showed a large range of charge carrier anisotropy, with these ratios ranging from 1 to over 690, as shown in Table 1. These particular

conditions warranted looking at the thin film properties to understand the attributes that contribute to charge carrier anisotropy.

Table 1. 6 selected conditions for Polybot that exhibit a range of anisotropic charge charrier characteristics that were discovered during the automated experimental workflow. Hole mobility (μ_h) expressed in units of $cm^2V^{-1}s^{-1}$.

Condition Number	Velocity (mm/s)	Temperature (C°)	Mobility (Parallel)	Mobility (Perpendicular)	Ratio (Para/Perp)	Optical Dichroic Ratio
1	10	50	0.015092	0.01434	1.052442	0.960997
2	9.5	50	0.010593	0.008191	1.293133	1.091078
3	10	40	0.006466	0.002459	2.630079	1.20054
4	9	50	0.012071	0.001328	9.090423	1.259301
5	0.9	30	0.00977	0.000308	31.76544	1.334722
6	1	45	0.004519	6.54E-06	690.6067	3.640845

To probe for the influence of solvent selection on processing of the hydrogen bond containing polymer, cryo-electron microscopy (cryo-EM) was utilized.[47] This technique was used to directly probe for the solution state aggregation of the polymer, and the results are depicted in **Figure 4A**. Samples were prepared from a 10 mg/mL chloroform solution of the polymer, which was flash frozen at -170°C, upon which images were taken of the polymer solution aggregates. It was observed that polymer in chloroform aggregates into particle-like domains when dissolved, which could potentially be attributed to intermolecular hydrogen bonding.[48] Notably, the formation of these aggregates in solution is often sought after for blade-coating applications towards generating anisotropic solid-state structures in thin films, both for enhancing electronic and thermomechanical performance.[49,50] These observations suggest that the combination of hydrogen bonding structure in combination with chloroform solvent complimented each other in developing

the charge anisotropic phenomena associated with blade-coating. These results were further complemented by FTIR analysis of drop-casted films of the polymer as shown in Figure SX, which was shown to have a split peak centered at roughly 3300 cm^{-1}, which correlates to the N-H stretching of the amide containing side chains, which can be attributed to both the bonded and non-bonded amide through intermolecular hydrogen bonding.

Following this analysis, characterizations on the films themselves were conducted to look at the solid-state material properties. One of the simplest ways to quantify degree of film alignment is by measuring the optical dichroic ratio from optical absorption measurements acquired in directions parallel and perpendicular to the direction of blade coating. Thus, cross polarized UV-vis was carried out on PTS-modified glass substrates that were coated using the Polybot with conditions identical to those used in measuring OFET carrier mobility of the 6 selected conditions of increasing anisotropy.

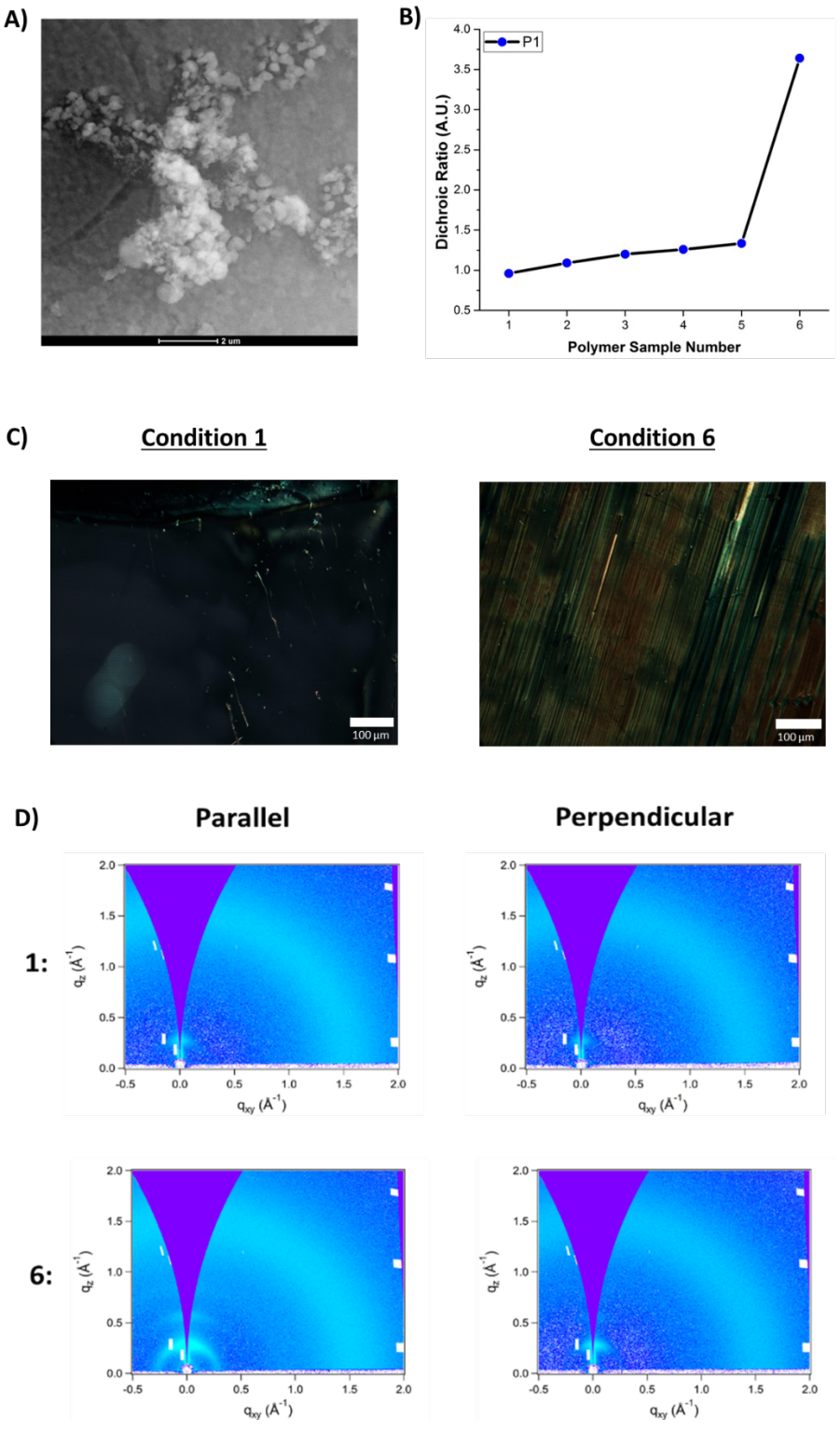

Figure 4. A) Cryo-EM image of polymer in 10mg/mL CHCl3 at 2µm. B) UV-Vis dichroic ratio of conditions 1-6. C) POM Image of Condition 1 and Condition 6 of thin films perpendicular to

coating direction. D) GIWAXS of Condition 1 and Condition 6 perpendicular and parallel to coating direction.

The degree of alignment of the polymer backbones within the overall thin film structure can be quantified using the dichroic ratio of the maximum absorbance between the polarized light parallel (0°) and perpendicular (90°) to the blade coating direction. Notably, as shown in Figure 4B which contains a plot of optical dichroic ratio vs the processing condition number, there is a trend between increasing dichroic ratio and anisotropic charge transport, which is more elaborated upon in the Table S1 and Figure SX. These observations indicate that polymer chain alignment plays a role in the observed electronic properties of the materials. Furthermore, increasing anisotropic conditions were consistently observed to have higher absorbance in the parallel blade coating direction, implying that the polymer chains align preferentially in direction of blade coating rather than perpendicular to it.[51]

To further clarify if anisotropic related chain alignment played a role in the electronic properties of the 6 selected conditions, polarized optical microscopy (POM) was performed on the thin films of the 6 samples to determine any variance in the optical birefringence, which can provide a qualitative measure of polymer chains alignment in conjugated polymers and other organic semiconductors, with conditions 1 and 6 which showed the lowest and highest degree of charge anisotropy show in **Figure 4C-D** respectively.[52] This phenomenon is correlated to the electric polarizability and transition dipole moment of the conjugated π-electron system being parallel to chain direction, thus readily being able to interact with polarized light for visual observation. At 90° polarized light (aligned to the direction parallel to the blade-coating), a trend was observed with increasing long-range alignment that could be positively correlated to higher degrees of charge anisotropy, as shown in **Figure 4C-D** (and further evidenced in Figure SX).

Condition 6 exhibited the highest degree of alignment when observed under POM, further indicating that alignment in the thin film plays a role in electronic anisotropic properties.[53,54] In compliment to this, atomic force microscopy (AFM) of the 6 conditions was also undertaken as shown in Figure SX. Interestingly, no notable trends or aligned fibers, typical morphologies associated with anisotropic charge transport, are observed in the selected conditions. Nonetheless, conditions 5 and 6 were observed to exhibit nondirectional fibrous morphologies as shown in Figure SXE and Figure SXF, indicating that the formation of microstructures in the thin film morphology does contribute to anisotropic electronic character observed in conditions 5 and 6.

To further get insight on the nanoscale morphology, grazing incidence wide-angle X-ray scattering (GIWAXS) was used to probe for the crystallinity of the thin films both parallel and perpendicular to the blade coating direction of the 6 conditions, as shown for Conditions 1 and 6 for **Figure 4D** and in Figure SX. Notably, as charge anisotropy increases, particularly with Condition 6, higher order peaks q_z peaks appear more prominently in the direction parallel to blade coating in comparison to the directions perpendicular to blade coating, indicating that crystallinity shows more prominence in the longer ranger of order across the blade coating direction, which is consistent with other reports of aligned conjugated polymer thin films.[55] Furthermore, arcing is seen in the parallel direction in comparison to the perpendicular one, indicating a broader distribution of crystallites across the long-range order, which is also consistent with other reports of aligned polymer films and indicates that the potential fibers along the parallel blade coating direction have significant size distribution.[49,56] Nonetheless, these results indicate that thin film crystallinity has a correlation with anisotropic charge transport in the hydrogen bonding based system, and that through careful screening of processing conditions, it is possible to control film crystallinity as well as other solid-state properties.

Conclusion

In conclusion, an automated blade-coating robotic platform was utilized to screen and analyze a variety of conditions for a hydrogen bonding containing DPP-based conjugated polymer. Using an automated high-throughput OFET fabrication platform, a wide range of processing conditions were investigated that varied both substrate temperature and blade-coating velocity towards measuring charge transport in both the parallel and perpendicular direction to blade-coating. Upon analysis of 30 different device fabrication conditions, it was possible to determine relationships between blade coating velocity and substrate temperature and electronic performance. Furthermore, through analysis of comparing electronic performances parallel and perpendicular to the direction of blade-coating, additional trends were discovered that demonstrated the possibility of controlling the degree of which charge carrier anisotropy occurred within the material, providing a potential avenue for fine tuning the electronic properties and solid-state morphology of the conjugated polymer. Furthermore, through these experiments, it was possible to uncover a processing condition with a substrate temperature of 45°C and a blade-coating speed of 1 mm/s that led to a very high anisotropic charge transport with a ratio as high as 690. In understanding the implications of these findings, 6 key conditions whose anisotropic charge transport ratios varied between 1 and 690 were selected and subsequently characterized for solid-state analysis. By using techniques such as GIWAXS, polarized UV-Vis and POMs it was found that the anisotropic electronic properties of the films were qualitatively and quantitatively correlated to the thin film crystallinity, amorphous regions, and dipole transition alignment, ultimately revealing a positive correlation with long-range polymer chain alignment and charge transport anisotropy. Overall, these observations are indicative that by using automation to screen for a wide range of processing conditions, it is possible to investigate novel interactions such as

hydrogen bonding in conjugated systems and thoroughly investigate their full potential, such as in this case where it can act as a powerful tool for inducing chain alignment and anisotropic charge transport. Future work will look at investigating other hydrogen bonding systems as well as further optimization of electronic performance towards developing next generation technologies through automated fabrication.

REFERENCES

(1) Berggren, M.; Nilsson, D.; Robinson, N. D. Organic Materials for Printed Electronics. *Nat. Mater.* **2007**, *6*, 3–5.

(2) Heremans, P.; Tripathi, A. K.; de Jamblinne de Meux, A.; Smits, E. C. P.; Hou, B.; Pourtois, G.; Gelinck, G. H. Mechanical and Electronic Properties of Thin-Film Transistors on Plastic, and Their Integration in Flexible Electronic Applications. *Adv. Mater.* **2016**, *28*, 4266–4282.

(3) Rogers, J. A. Electronics for the Human Body. *J. Am. Med. Assoc.* **2015**, *313*, 561–562.

(4) O 'connor, T. F.; Rajan, K. M.; Printz, A. D.; Lipomi, D. J. Toward Organic Electronics with Properties Inspired by Biological Tissue. *J. Mater. Chem. B* **2015**, *3*, 4947–4952.

(5) Kaloni, T. P.; Giesbrecht, P. K.; Schreckenbach, G.; Freund, M. S. Polythiophene: From Fundamental Perspectives to Applications. *Chem. Mater.* **2017**, *29*, 10248–10283.

(6) Mooney, M.; Nyayachavadi, A.; Rondeau-Gagné, S. Eco-Friendly Semiconducting Polymers: From Greener Synthesis to Greener Processability. *J. Mater. Chem. C* **2020**.

(7) Lee, E. K.; Lee, M. Y.; Park, C. H.; Lee, H. R.; Oh, J. H. Toward Environmentally Robust Organic Electronics: Approaches and Applications. *Adv. Mater.* **2017**, *29*, 1–29.

(8) Ocheje, M. U.; Charron, B. P.; Nyayachavadi, A.; Rondeau-Gagné, S. Stretchable Electronics: Recent Progress in the Preparation of Stretchable and Self-Healing Semiconducting Conjugated Polymers. *Flex. Print. Electron.* **2017**, *2*, 043002.

(9) Ling, M. M.; Bao, Z. Thin Film Deposition, Patterning, and Printing in Organic Thin Film Transistors. *Chem. Mater.* **2004**, *16*, 4824–4840.

(10) Yao, Y.; Dong, H.; Hu, W. Charge Transport in Organic and Polymeric Semiconductors for Flexible and Stretchable Devices. *Adv. Mater.* **2016**, *28*, 4513–4523.

(11) Mei, J.; Bao, Z. Side Chain Engineering in Solution-Processable Conjugated Polymers. *Chem. Mater.* **2014**, *26*, 604–615.

(12) Luo, N.; Ren, P.; Feng, Y.; Shao, X.; Zhang, H. L.; Liu, Z. Side-Chain Engineering of Conjugated Polymers for High-Performance Field-Effect Transistors. *J. Phys. Chem. Lett.* **2022**, *13*, 1131–1146.

(13) Wang, G. J. N.; Shaw, L.; Xu, J.; Kurosawa, T.; Schroeder, B. C.; Oh, J. Y.; Benight, S. J.; Bao, Z. Inducing Elasticity through Oligo-Siloxane Crosslinks for Intrinsically Stretchable Semiconducting Polymers. *Adv. Funct. Mater.* **2016**, *26*, 7254–7262.

(14) Yang, H.; Yuan, B.; Zhang, X.; Scherman, O. A. Supramolecular Chemistry at Interfaces: Host-Guest Interactions for Fabricating Multifunctional Biointerfaces. *Acc. Chem. Res.* **2014**, *47*, 2106–2115.

(15) Mooney, M.; Wang, Y.; Nyayachavadi, A.; Zhang, S.; Gu, X.; Rondeau-Gagné, S. Enhancing the Solubility of Semiconducting Polymers in Eco-Friendly Solvents with Carbohydrate-Containing Side Chains. *ACS Appl. Mater. Interfaces* **2021**, *13*, 25175–

25185.

(16) Lv, S.; Li, L.; Mu, Y.; Wan, X. Side-Chain Engineering as a Powerful Tool to Tune the Properties of Polymeric Field-Effect Transistors. *Polym. Rev.* **2021**, *61*, 520–552.

(17) Lee, M. H.; Kang, M.; Jeong, H. G.; Park, J. J.; Hwang, K.; Kim, D. Y. Effect of Semi-Fluorinated Alkyl Side Chains on Conjugated Polymers with Planar Backbone in Organic Field-Effect Transistors. *Macromol. Rapid Commun.* **2018**, *39*, 1–7.

(18) Welterlich, I.; Tieke, B. Conjugated Polymer with Benzimidazolylpyridine Ligands in the Side Chain: Metal Ion Coordination and Coordinative Self-Assembly into Fluorescent Ultrathin Films. *Macromolecules* **2011**, *44*, 4194–4203.

(19) Mei, J.; Kim, D. H.; Ayzner, A. L.; Toney, M. F.; Bao, Z. Siloxane-Terminated Solubilizing Side Chains: Bringing Conjugated Polymer Backbones Closer and Boosting Hole Mobilities in Thin-Film Transistors. *J. Am. Chem. Soc.* **2011**, *133*, 20130–20133.

(20) Shih, H. K.; Chen, Y. H.; Chu, Y. L.; Cheng, C. C.; Chang, F. C.; Zhu, C. Y.; Kuo, S. W. Photo-Crosslinking of Pendent Uracil Units Provides Supramolecular Hole Injection/Transport Conducting Polymers for Highly Efficient Light-Emitting Diodes. *Polymers (Basel).* **2015**, *7*, 804–818.

(21) Lin, Y. C.; Chen, C. K.; Chiang, Y. C.; Hung, C. C.; Fu, M. C.; Inagaki, S.; Chueh, C. C.; Higashihara, T.; Chen, W. C. Study on Intrinsic Stretchability of Diketopyrrolopyrrole-Based π-Conjugated Copolymers with Poly(Acryl Amide) Side Chains for Organic Field-Effect Transistors. *ACS Appl. Mater. Interfaces* **2020**, *12*, 33014–33027.

(22) Ye, L.; Pankow, R. M.; Horikawa, M.; Melenbrink, E. L.; Liu, K.; Thompson, B. C. Green-

Solvent-Processed Amide-Functionalized Conjugated Polymers Prepared via Direct Arylation Polymerization (DArP). *Macromolecules* **2019**, *52*, 9383–9388.

(23) Yang, K.; He, T.; Chen, X.; Cheng, S. Z. D.; Zhu, Y. Patternable Conjugated Polymers with Latent Hydrogen-Bonding on the Main Chain. *Macromolecules* **2014**, *47*, 8479–8486.

(24) Gao, Y.; Zhang, X.; Tian, H.; Zhang, J.; Yan, D.; Geng, Y.; Wang, F. High Mobility Ambipolar Diketopyrrolopyrrole-Based Conjugated Polymer Synthesized Via Direct Arylation Polycondensation. *Adv. Mater.* **2015**, *27*, 6753–6759.

(25) Głowacki, E. D.; Irimia-Vladu, M.; Bauer, S.; Sariciftci, N. S. Hydrogen-Bonds in Molecular Solids-from Biological Systems to Organic Electronics. *J. Mater. Chem. B* **2013**, *1*, 3742–3753.

(26) Galuska, L. A.; Ocheje, M. U.; Ahmad, Z. C.; Rondeau-Gagné, S.; Gu, X. Elucidating the Role of Hydrogen Bonds for Improved Mechanical Properties in a High-Performance Semiconducting Polymer. *Chem. Mater.* **2022**, *34*, 2259–2267.

(27) Xu, Z.; Park, K. S.; Diao, Y. What Is the Assembly Pathway of a Conjugated Polymer From Solution to Thin Films? *Front. Chem.* **2020**, *8*, 1–9.

(28) Ma, H.; Yip, H. L.; Huang, F.; Jen, A. K. Y. Interface Engineering for Organic Electronics. *Adv. Funct. Mater.* **2010**, *20*, 1371–1388.

(29) Yao, Y.; Dong, H.; Hu, W. Ordering of Conjugated Polymer Molecules: Recent Advances and Perspectives. *Polym. Chem.* **2013**, *4*, 5197–5205.

(30) Mullin, W. J.; Sharber, S. A.; Thomas, S. W. Optimizing the Self-Assembly of Conjugated Polymers and Small Molecules through Structurally Programmed Non-Covalent Control. *J.*

Polym. Sci. **2021**, *59*, 1643–1663.

(31) Chang, M.; Lim, G. T.; Park, B.; Reichmanis, E. Control of Molecular Ordering, Alignment, and Charge Transport in Solution-Processed Conjugated Polymer Thin Films. *Polymers (Basel).* **2017**, *9*, 23–31.

(32) Ocheje, M. U.; Charron, B. P.; Cheng, Y.-H.; Chuang, C.-H.; Soldera, A.; Chiu, Y.-C.; Rondeau-Gagné, S. Amide-Containing Alkyl Chains in Conjugated Polymers: Effect on Self-Assembly and Electronic Properties. *Macromolecules* **2018**, *51*, 1336–1344.

(33) Ocheje, M. U.; Selivanova, M.; Zhang, S.; Van Nguyen, T. H.; Charron, B. P.; Chuang, C. H.; Cheng, Y. H.; Billet, B.; Noori, S.; Chiu, Y. C.; Gu, X.; Rondeau-Gagné, S. Influence of Amide-Containing Side Chains on the Mechanical Properties of Diketopyrrolopyrrole-Based Polymers. *Polym. Chem.* **2018**, *9*, 5531–5542.

(34) Dong, H.; Li, H.; Wang, E.; Wei, Z.; Xu, W.; Hu, W.; Yan, S. Ordering Rigid Rod Conjugated Polymer Molecules for High Performance Photoswitchers. *Langmuir* **2008**, *24*, 13241–13244.

(35) Callaway, C. P.; Liu, A. L.; Venkatesh, R.; Zheng, Y.; Lee, M.; Meredith, J. C.; Grover, M.; Risko, C.; Reichmanis, E. The Solution Is the Solution: Data-Driven Elucidation of Solution-to-Device Feature Transfer for π-Conjugated Polymer Semiconductors. *ACS Appl. Mater. Interfaces* **2022**, *14*, 3613–3620.

(36) Choi, H. H.; Cho, K.; Frisbie, C. D.; Sirringhaus, H.; Podzorov, V. Critical Assessment of Charge Mobility Extraction in FETs. *Nat. Mater.* **2017**, *17*, 2–7.

(37) Evans, R. C. Harnessing Self-Assembly Strategies for the Rational Design of Conjugated

Polymer Based Materials. *J. Mater. Chem. C* **2013**, *1*, 4190–4200.

(38) Stupp, S. I.; Palmer, L. C. Supramolecular Chemistry and Self-Assembly in Organic Materials Design. *Chem. Mater.* **2014**, *26*, 507–518.

(39) Ocheje, M. U.; Charron, B. P.; Cheng, Y. H.; Chuang, C. H.; Soldera, A.; Chiu, Y. C.; Rondeau-Gagné, S. Amide-Containing Alkyl Chains in Conjugated Polymers: Effect on Self-Assembly and Electronic Properties. *Macromolecules* **2018**, *51*, 1336–1344.

(40) Charron, B. P.; Ocheje, M. U.; Selivanova, M.; Hendsbee, A. D.; Li, Y.; Rondeau-Gagné, S. Electronic Properties of Isoindigo-Based Conjugated Polymers Bearing Urea-Containing and Linear Alkyl Side Chains. *J. Mater. Chem. C* **2018**, *6*, 12070–12078.

(41) Shi, X.; Bao, W. Hydrogen-Bonded Conjugated Materials and Their Application in Organic Field-Effect Transistors. *Front. Chem.* **2021**, *9*, 1–6.

(42) Kimpel, J.; Michinobu, T. Conjugated Polymers for Functional Applications: Lifetime and Performance of Polymeric Organic Semiconductors in Organic Field-Effect Transistors. *Polym. Int.* **2021**, *70*, 367–373.

(43) Yan, Y.; Huang, J.; Tang, B. Z. Kinetic Trapping-a Strategy for Directing the Self-Assembly of Unique Functional Nanostructures. *Chem. Commun.* **2016**, *52*, 11870–11884.

(44) Shao, B.; Zhu, X.; Plunkett, K. N.; Vanden Bout, D. A. Controlling the Folding of Conjugated Polymers at the Single Molecule Level: Via Hydrogen Bonding. *Polym. Chem.* **2017**, *8*, 1188–1195.

(45) Biniek, L.; Pouget, S.; Djurado, D.; Gonthier, E.; Tremel, K.; Kayunkid, N.; Zaborova, E.; Crespo-Monteiro, N.; Boyron, O.; Leclerc, N.; Ludwigs, S.; Brinkmann, M. High-

Temperature Rubbing: A Versatile Method to Align π-Conjugated Polymers without Alignment Substrate. *Macromolecules* **2014**, *47*, 3871–3879.

(46) Wang, M.; Baek, P.; Akbarinejad, A.; Barker, D.; Travas-Sejdic, J. Conjugated Polymers and Composites for Stretchable Organic Electronics. *J. Mater. Chem. C* **2019**, *7*, 5534–5552.

(47) Li, Y.; Huang, W.; Li, Y.; Chiu, W.; Cui, Y. Opportunities for Cryogenic Electron Microscopy in Materials Science and Nanoscience. *ACS Nano* **2020**, *14*, 9263–9276.

(48) González-Rodríguez, D.; Schenning, A. P. H. J. Hydrogen-Bonded Supramolecular π-Functional Materials. *Chem. Mater.* **2011**, *23*, 310–325.

(49) Pandey, M.; Kumari, N.; Nagamatsu, S.; Pandey, S. S. Recent Advances in the Orientation of Conjugated Polymers for Organic Field-Effect Transistors. *J. Mater. Chem. C* **2019**, *7*, 13323–13351.

(50) Qu, G.; Zhao, X.; Newbloom, G. M.; Zhang, F.; Mohammadi, E.; Strzalka, J. W.; Pozzo, L. D.; Mei, J.; Diao, Y. Understanding Interfacial Alignment in Solution Coated Conjugated Polymer Thin Films. *ACS Appl. Mater. Interfaces* **2017**, *9*, 27863–27874.

(51) Kim, N.-K.; Jang, S.; Pace, G.; Caironi, M.; Park, W.-T.; Khim, D.; Kim, J.; Kim, D.; Noh, Y. High-Performance Organic Field-Effect Transistors with Directionally Aligned Conjugated Polymer Film Deposited from Pre-Aggregated Solution. *Chem. Mater.* **2015**, *27*, 8345–8353.

(52) Koynov, K.; Bahtiar, A.; Ahn, T.; Bubeck, C.; Hörhold, H. H. Molecular Weight Dependence of Birefringence of Thin Films of the Conjugated Polymer Poly[2-Methoxy-5-

(2′-Ethyl-Hexyloxy)-1, 4-Phenylenevinylene]. *Appl. Phys. Lett.* **2004**, *84*, 3792–3794.

(53) Zhao, Y.; Gumyusenge, A.; He, J.; Qu, G.; McNutt, W. W.; Long, Y.; Zhang, H.; Huang, L.; Diao, Y.; Mei, J. Continuous Melt-Drawing of Highly Aligned Flexible and Stretchable Semiconducting Microfibers for Organic Electronics. *Adv. Funct. Mater.* **2018**, *28*, 1–9.

(54) Müller, C.; Aghamohammadi, M.; Himmelberger, S.; Sonar, P.; Garriga, M.; Salleo, A.; Campoy-Quiles, M. One-Step Macroscopic Alignment of Conjugated Polymer Systems by Epitaxial Crystallization during Spin-Coating. *Adv. Funct. Mater.* **2013**, *23*, 2368–2377.

(55) Kim, C.; Joung, H.; Kim, H. J.; Paeng, K.; Kaufman, L. J.; Yang, J. Aggregates of Conjugated Polymers : Bottom-up Control of Mesoscopic Morphology and Photophysics. **2023**, 1–13.

(56) Kim, Y. J.; Lee, S.; Niazi, M. R.; Hwang, K.; Tang, M. C.; Lim, D. H.; Kang, J. S.; Smilgies, D. M.; Amassian, A.; Kim, D. Y. Systematic Study on the Morphological Development of Blade-Coated Conjugated Polymer Thin Films via in Situ Measurements. *ACS Appl. Mater. Interfaces* **2020**, *12*, 36417–36427.

ASSOCIATED CONTENT

Supporting Information.

Author Information

Corresponding Author

*E-mail: srondeau@uwindsor.ca (S.R.-G.)

xuj@anl.gov (J.X.)

ORCID

Simon Rondeau-Gagné: 0000-0003-0487-1092

Author Contributions

All authors contributed to the manuscript. All authors have given approval to the final version of the manuscript.

Funding

This work was supported by NSERC through a Discovery Grants RGPIN-2022-04428 (S.R.-G.). A.N. and M.M. thank NSERC for financial support through a NSERC Postgraduate Scholarship – Doctoral. Y.W. and X.G. are thankful for the financial support from NSF (DMR-2047689) for enabling the X-ray based morphology characterization of thin films in this work.

Notes:

The authors declare no competing financial interest.

ACKNOWLEDGMENT

The authors thank Dr. Matt Revington (UWindsor) for assistance conducting NMR studies. The authors also thank Jacob G. Rothera for assistance with the POM measurements.